Progress In Electromagnetics Research B, Vol. 54, 303–319, 2013

BLUETOOTH/UWB DUAL-BAND PLANAR DIVERSITY ANTENNA WITH WiMAX AND WLAN BAND-NOTCH CHARACTERISTICS

Gopi S. Reddy[1, *], Ashish Chittora[1], Shilpa Kharche[1], Sanjeev Mishra[2], and Jayanta Mukherjee[1]

[1]Department of Electrical Engineering, Indian Institute of Technology (IIT) Bombay, Mumbai 400076, India

[2]Department of Avionic, Indian Institute of Space Science and Technology (IIST) Trivandrum, India

Abstract—In this paper, a stage wise realization of compact Bluetooth — UWB dual-band diversity antenna with WiMAX and WLAN band-notch characteristics is presented. The proposed structure consists of two co-planar semicircular dual band-notch monopole antennas, mounted with planar spiral. Individual antenna configuration provides an impedance bandwidth (VSWR < 2) for dual-band i.e., both Bluetooth and UWB bands. For dual band-notch characteristic, two sets of spirals are capacitively coupled with the feed line of antenna. This configuration provides band-notch (VSWR < 2) for WiMAX i.e., (3.3–3.6 GHz) and WLAN (5.13–5.85 GHz) bands. For enhancing reception capabilities of the proposed structure, twin coplanar antennas are used to fulfill diversity requirements. However, due to coplanar and close proximity to each other, there is high possibility of mutual coupling between coplanar antenna elements. To address the mutual coupling between elements, cross-strip variable-sized frequency selective structures are used. Antenna diversity of the proposed structure is validated by measuring radiation pattern characteristic and envelop co-relation factor (ECC). A good agreement between measured and simulated responses ensures that the proposed diversity antenna can be used for interference free Bluetooth/UWB dual-band applications.

Received 4 August 2013, Accepted 12 September 2013, Scheduled 16 September 2013

* Corresponding author: Gopi Shrikanth Reddy (shri@ee.iitb.ac.in).

1. INTRODUCTION

With declaration of 3.1 to 10.6 GHz as an unlicensed band by Federal communication commission (FCC) [1], a tremendous amount of research interest is focused in the area of Ultra wideband (UWB) technology. However, even with tremendous advantages and possibilities, UWB systems faces many implementation challenges. Apart from compactness, other major challenges related to implementation of UWB systems are co-channel interference and multi-path fading. Co-channel interference in UWB system is due to co-existing narrow frequency bands, such as WiMAX (3.3–3.6 GHz) and WLAN (5.12–5.3 GHz and 5.75–5.83 GHz). Seeking these issues it is desirable that antenna integrated in UWB systems should be compact and exhibit multi band-notch characteristic with pattern diversity.

Recently, many multi band-notch antenna configurations have been proposed [2–9]. Most common techniques for attaining multi band-notch characteristic are slot techniques and open or close ended loop resonator techniques. Slot technique involves etching of quarter or half wave length slots on antenna or ground plane [2–6]. Though effective, slot techniques are limited to single or dual band-notch only. For multi band-notch, multiple slots can be utilized [4–6], but it will affect antenna's performance in terms of decrement in antenna's gain and efficiency. On the other hand, open or close loop techniques involve capacitive or inductive coupling of quarter or half wavelength open or closed planar loops resonators with antenna feed line, with radiator [7, 8] or with the ground plan [9]. These techniques brilliantly exhibit multi band-notch characteristics without affecting antenna performance. These loop structures are self resonant structures and provide sharp resonance at the frequency for which they are designed. Due to their out-of-phase resonant behaviour they cancel out the surface currents at ground plane and feed line, which provides sharp band-notch characteristics.

For addressing multipath fading issue it is desirable that antennas for short range communication should possesses diversity characteristic. Antenna diversity involves coplanar twin antenna system with separate feeds [10–14], this enhances reception capability of antenna and increases antenna gain. Since it has coplanar-twin antennas, it is important that there should be minimum mutual coupling between them. Mutual coupling can be reduced by maintaining specific distance between coplanar antennas, but for UWB systems where compactness is a requirement, other methodologies have to be adopted. In [12, 15, 16] reported structures involve slots, Electromagnetic Band Gap structures (EBG), and parasitic strips for

reduction in mutual coupling. However these techniques are confined to narrow or broad band only.

In this paper, realization of the proposed antenna is done in two stages. First stage involves designing of Bluetooth/UWB dual-band antenna using semicircular monopole with planar spiral mounted on it and dual-band notch characteristics using a set of capacitively coupled spiral. In second stage pattern diversity antenna configuration is realized by using twin coplanar antennas (of stage one) separated by cross-striped variable sized frequency selective structure (VFSS). This configuration provides high isolation of $|S_{21}| < -25$ dB with good pattern diversity. This paper is organized in four sections. Section 2 explains stage 1 i.e., realization of dual-band antenna with dual band-notch characteristic. Section 3 explains stage 2 i.e., realization of twin coplanar dual-band antenna with diversity and reduced mutual coupling. Finally Section 4 gives the conclusions. Experimental and theoretical verifications were carried out in every section. For optimisation and theoretical analysis, finite integral transform (FIT) based CST Microwave studio simulation software is used.

2. COMPACT DUAL BAND ANTENNA WITHOUT AND WITH DUAL-BAND NOTCH CHARACTERISTIC (STAGE 1)

2.1. Integrated Bluetooth/UWB Dual-band Antenna

The proposed structure, as shown in Figure 1, consists of a simple semicircular monopole with a regular planar spiral (Sp_1) mounted on it. Due to the addition of spiral shape, overall size of the proposed antenna is less than other dual-band configurations reported in [17–20]. The proposed structure is designed on RT Duriod 5880 substrate with $\varepsilon_r = 2.2$, $\tan\delta = 0.0009$ and 0.787 mm thickness. The total surface area of the proposed base antenna is $(L_{sub} \times W_{sub})$ $24 \times 17\,\text{mm}^2$. Dimensional values of this semicircular monopole are calculated using design considerations given in [21]. To achieve desired Bluetooth bandwidth, a planar spiral (Sp_1) is mounted on semicircular monopole at a distance a'. For approximating the number of turns in Sp_1, empirical equations given in [22] are used as:

$$L_{total} = \frac{4L_{out}N - [2N(1+N) - 3](s + w_1)}{N} \tag{1}$$

$$N_{normalized} = \text{integer part of} \left[\frac{L_{out} - (s + w_1)}{2(s + w_1)} \right] \tag{2}$$

Here N is number of turns, L_{out} the side length of outer turn, s the gap between turns, w_1 the width of spiral strip, and L_{total} the total

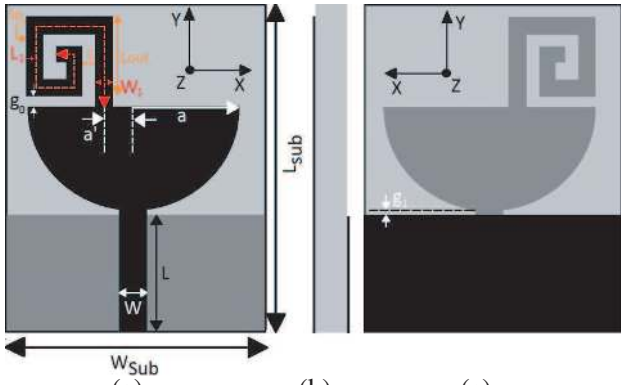

Figure 1. The proposed dual-band base antenna, (a) front view, (b) side view, (c) back view.

effective length i.e., L_1 of Sp_1 which is approximated as:

$$L_{total} \approx L_1 \approx L_{eff} \approx \frac{c}{4f_c\sqrt{\varepsilon_{reff}}} \approx \frac{\lambda_g}{4} \tag{3}$$

i.e., Quarter of guided wavelength (λ_g). Here c is the speed of light in free space and ε_{reff} the effective dielectric constant. Since for Bluetooth application, resonating frequency (f_c) is 2.45 GHz, the effective length ($L_{total} = L_{eff}$) according to Equation (3) should be 22.791 mm. Apart from L_{total} in Equation (1), L_{out}, S and w_1 are also needed for calculating number of turns (N) in spiral resonator. It can be seen in Equation (1) or (2) that as L_{out} increases so does the number of turns (N). With approximations of $S = w_1 = 1$ mm, relation between L_{out} and N is derived using Equations (1), (2) and represented graphically in Figure 2.

It can be seen that there is deviation between the curves, because Equation (2) gives a normalized value for number of turns. The graph in Figure 2 clearly depicts that as side length of outer turn is increased, number of turns (N) will also increase, and according to [22], inductance of a spiral reduces as the number of turns increases. So according to Figure 2, if $L_{out} < 7$ mm, N will be less than 1, and it will be complicated to accommodate 22.8 mm to get desired resonating frequency. Even with $L_{out} > 7$ mm, design complication will arise. Therefore, theoretically taking $L_{out} = 7$ mm, the number of turns (N) is approximated as 1.38. Based on these theoretical results, the dimensional values for the planar spiral are further optimized using simulation software. After optimization, the exact dimensional values

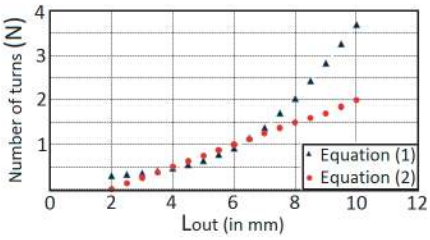

Figure 2. L_{out} Vs number of turns (N), here $L_{total} = 22.8\,\text{mm}$, $S = w_1 = 1\,\text{mm}$.

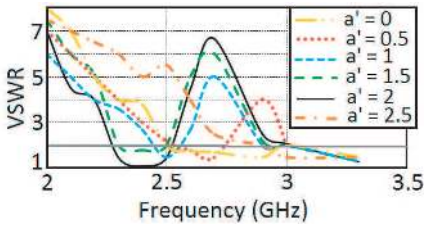

Figure 3. VSWR (impedance bandwidth) for different value of a'.

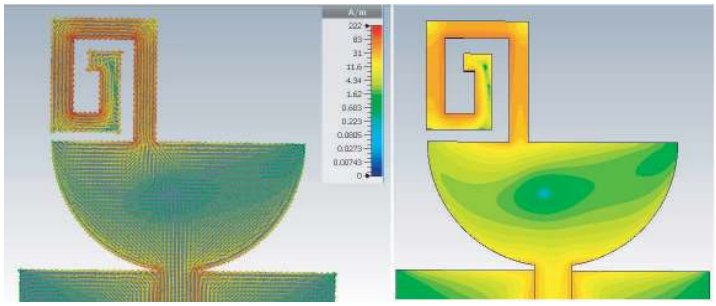

Figure 4. Vectored and absolute current distribution at 2.45 GHz.

for Sp_1 are: $L_1 = 31.5\,\text{mm}$, $L_{out} = 7\,\text{mm}$, $S = 1\,\text{mm}$, $w_1 = 1\,\text{mm}$. The deviations between theoretical and practical values (L_{eff} and L_1) are due to the fact that Sp_1 is attached to semicircular monopole rather than theoretical consideration of independently resonating spiral structure. Perfect impedance matching (VSWR < 2) for Bluetooth bandwidth is achieved by optimizing the value of a', as shown in Figure 3.

The current distribution shown in Figure 4 also validates the resonant behavior of Sp_1. After optimizing impedance bandwidth for Bluetooth band, the proposed base antenna is fabricated and tested. The optimized dimensions of the fabricated antenna are as: $N = 1.38$, $L_1 = 31.5$, $g_o = 0.5$, $S = 1$, $L_{out} = 7$, $w_1 = 1$, $a = 8$, $a' = 2$, $L = 7.5$, $W = 2.2$, $L_{sub} = 24$, $W_{sub} = 17$, $g_1 = 0.2$ (all dimensions are in mm).

Both simulated and measured results shown in Figure 5 confirm the desired dual-band characteristic of the proposed base antenna. The radiation plot shown in Figure 6 depicts that the proposed dual-band antenna exhibits a monopole like pattern for principle plans i.e., figure

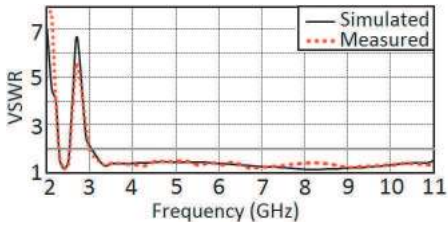

Figure 5. Simulated and measured VSWR characteristic of the proposed dual-band antenna.

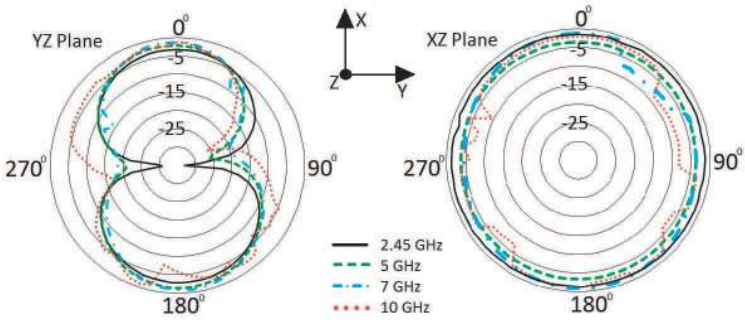

Figure 6. Measured radiation pattern (dB).

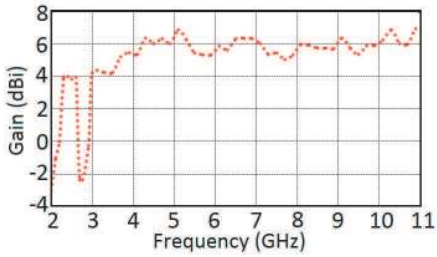

Figure 7. Measured gain response.

of eight pattern in YZ and omnidirectional pattern in XZ.

Compared to [19, 20], the proposed antenna posses a wide bandwidth and stable radiation pattern, even with its compact size. The measured gain response also validates the radiation stability of the proposed dual-band antenna.

The gain response shown in Figure 7 depicts a stable gain response with variations within 3 dBi for both the pass bands.

2.2. Dual-band Antenna with WiMAX, WLAN Band-notch Characteristic

In order to address interference issue, it is important that UWB antenna should have band rejection characteristic intrinsically. For achieving dual band-notch characteristics, a set of planar spirals Sp_2, Sp_3 are capacitively coupled with feed line, as shown in Figure 8.

Design procedure of Sp_2 and Sp_3 are similar to Sp_1, except the effective lengths of Sp_2 and Sp_3 are chosen as $\lambda_g/2$ i.e.,

$$L_{eff\,(3.45\,\mathrm{GHz},5.477\,\mathrm{GHz})} \approx \frac{C}{2f_c\sqrt{\varepsilon_{reff}}} \approx \frac{\lambda_g}{2} \tag{4}$$

The reason for choosing $\lambda_g/2$ (instead of $\lambda_g/4$) as effective length is to avoid fabrication difficulties especially for WLAN. As shown in Figure 6, Sp_3 is rectangular instead of square. This is because Sp_3 is designed to notch WLAN band, and since L_{out2} is approximated 4 mm, it is difficult to accommodate effective length of Sp_3, i.e., 20.41 mm ($\lambda_g/2$ for 5.477 GHz) using regular spiral structure. To achieve band notch for WLAN, Sp_3 is optimized with respect to its effective length and other dimensional parameters. Optimized effective lengths of Sp_2 and Sp_3 are 31 mm and 23 mm, respectively. Other optimized values are $L_{out1} = 6$, $w_2 = 1$, $S_1 = 1$, $L_{out2} = 4$, $L_{out2} = 6$, $S_2 = 0.5$, $w_3 = 1$ (all dimensions are in mm). For achieving sharp cutoff for notch bandwidths, gaps between feed line and spirals (g_1 and g_2) are also optimized.. Figure 9 shows the optimization of g_1 and g_2 vs VSWR characteristic.

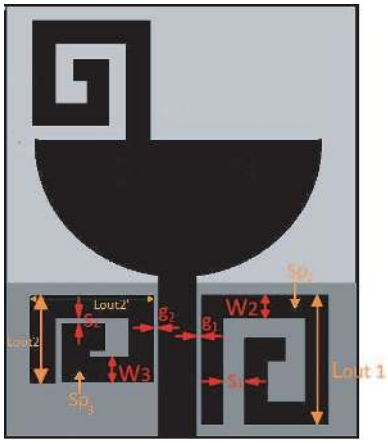

Figure 8. Configurations of dual-band antenna with WiMAX and WLAN characteristic.

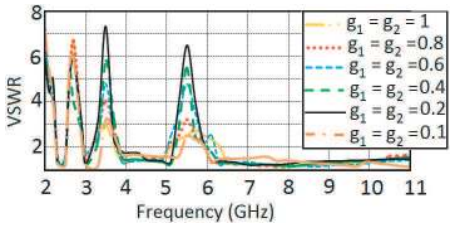

Figure 9. Optimisation of notch-bandwidth with respect to gap g_1 and g_2 (all dimensions are in mm).

Figure 9 shows that a sharp cutoff for notch bandwidths is achieved by adjusting the gaps between spirals and feed line. Due to its self-resonating property, each spiral (Sp_2 and Sp_3) provides an out of phase resonating current which cancels current across feed line and ground plane, resulting in sharp band-notch. This phenomenon can be seen in surface distribution characteristic shown in Figure 10.

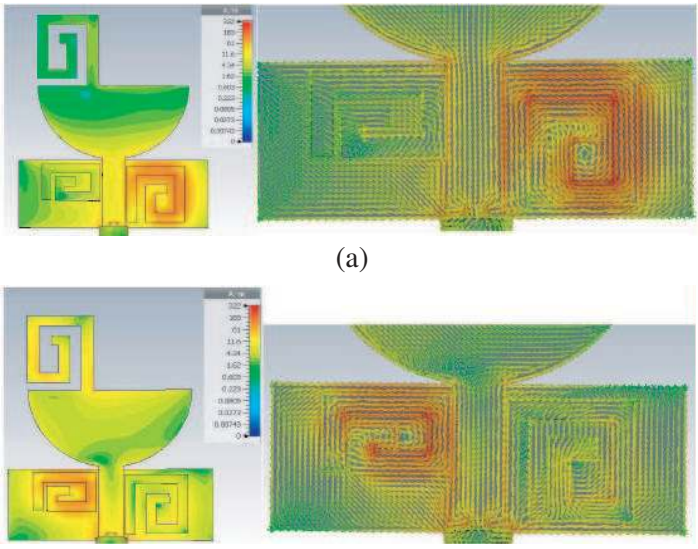

(a)

(b)

Figure 10. Current distribution at (a) 3.45 GHz, (b) 5.447 GHz.

Based on simulated results proposed dual-band antenna with band-notch is fabricated and tested. It can be seen in Figure 11 that both simulated and measured results are in good agreement.

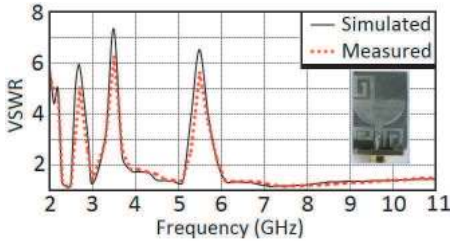

Figure 11. VSWR characteristics of Dual band Antenna with WiMAX and WLAN band-notch.

After ensuring the bandwidth response and dual-band notch characteristic of individual structure, proposed base antenna is combined with similar antenna (coplanar) to address diversity issue.

3. REALIZATION OF DIVERSITY ANTENNA WITH REDUCED MUTUAL COUPLING (STAGE 2)

For realizing antenna diversity aspect, the presented dual-band antenna with band-notch is combined with a similar antenna as shown in Figure 12. The distance between two antenna elements is optimized to nearly quarter wavelength ($\lambda_g/4$) of 2.45 GHz to maintain dual bandwidth. But due to this small distance, the mutual coupling between antenna elements is high.

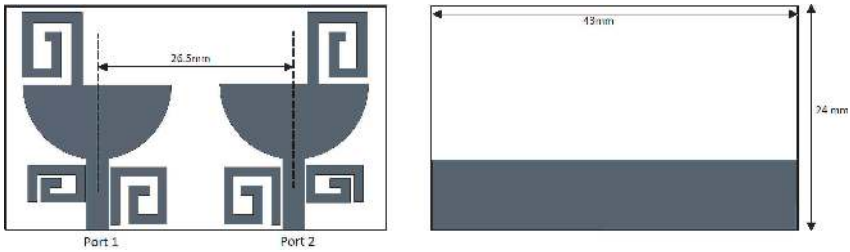

Figure 12. Twin coplanar antenna, (a) front view, (b) back view.

As depicted in Figure 13, the mutual coupling between antenna elements is high, and at certain frequencies it is beyond −15 dB. The mutual coupling between the elements can be reduced by increasing the inter-element separation to half wavelength ($\lambda_g/2$ i.e., within limits of avoiding grating lobe), but this will increase PCB size. In order

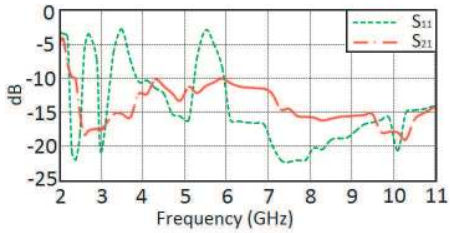

Figure 13. *S*-parameter of the proposed antenna (Figure 11).

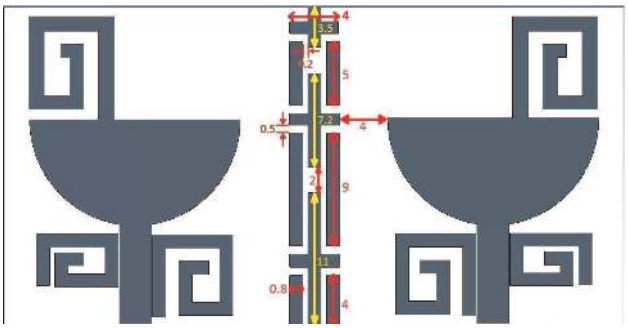

Figure 14. Proposed cross-strip VFSS structure for mutual coupling reduction (all dimensions are in mm).

to reduce mutual coupling without increasing inter-element spacing, EBG (Electromagnetic Band Gap) structures or Frequency selective surfaces (FSS) can be used, but due to their narrow band nature, they are not very effective for ultra wide bandwidth. To overcome this issue Variable-sized frequency selective structures (VFSS) are designed to overcome mutual coupling for ultra wide bandwidth.

As shown in Figure 14, VFSS structure consists of cross-strip lines along with parallel strip line. The lengths of these cross-strip lines (marked with yellow arrows) are optimized to nearly quarter wave length ($\lambda_g/4$) for 5 GHz, 7 GHz, and 10 GHz. VFSS consists of cross-strip lines with different resonant lengths, which are effective for ultra-wide bandwidth. The gaps between the inductive strip lines are optimised to generate surface current cancellation effect between intermediate strips. Working of the cross-strip structure is analysed through surface current distribution and *S*-parameter characteristics.

As depicted in Figure 15, with the introduction of cross-strip VFSS, the magnitude of surface current is reduced in another antenna. Transmission parameter (S_{21}) shown in Figure 16 also validates the

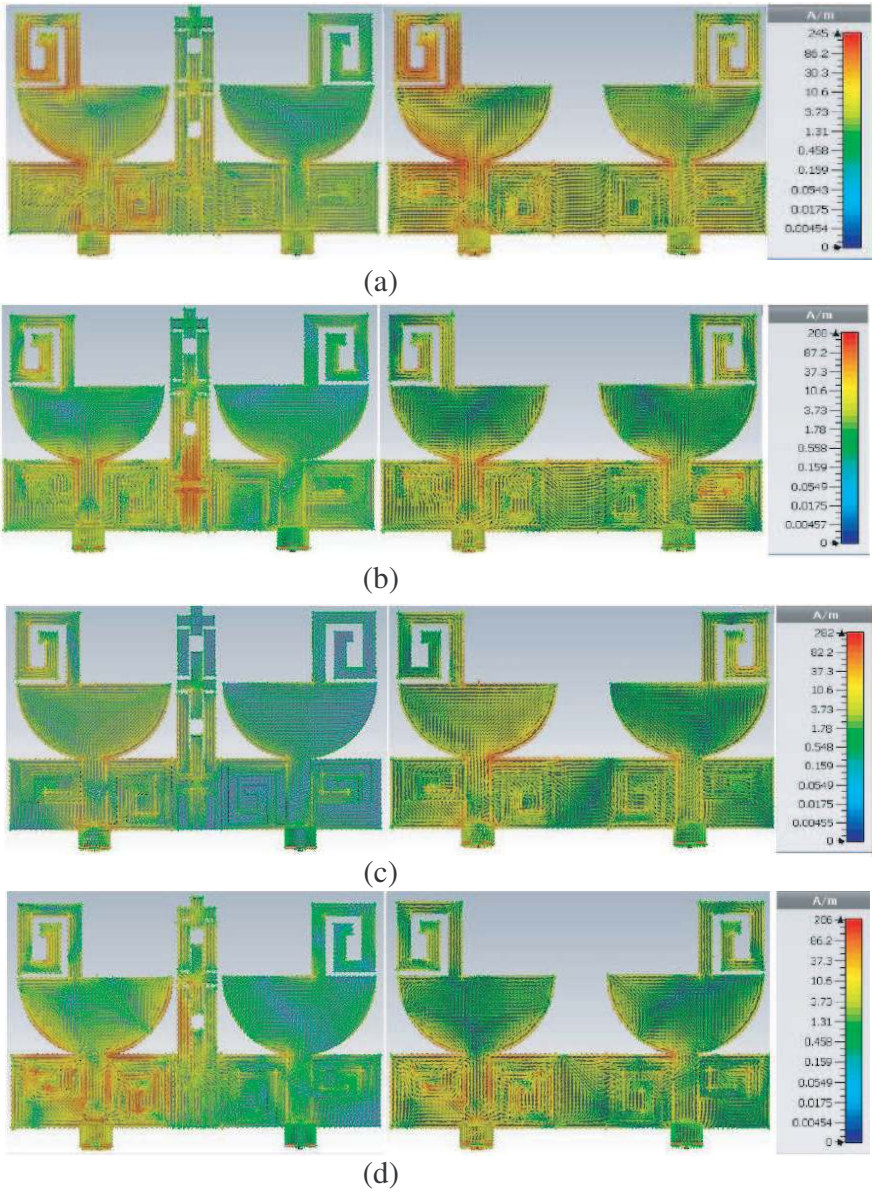

Figure 15. (Port 1) Surface current distribution of diversity antenna with and without cross-strip: (a) 2.45 GHz, (b) 5 GHz, (c) 7 GHz and (d) 10 GHz.

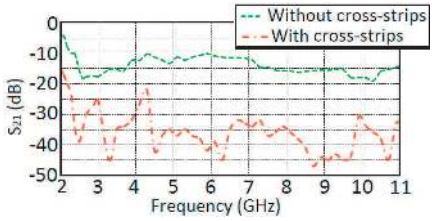

Figure 16. Comparison of transmission parameters (S_{21}).

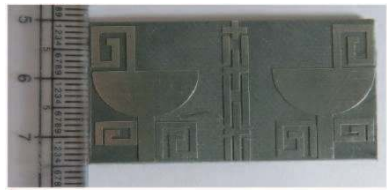

Figure 17. Fabricated antenna with cross-strip VFSS.

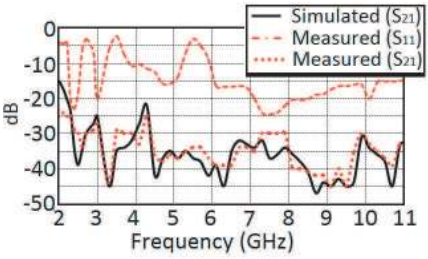

Figure 18. Measured S-parameter of antenna shown in Figure 17.

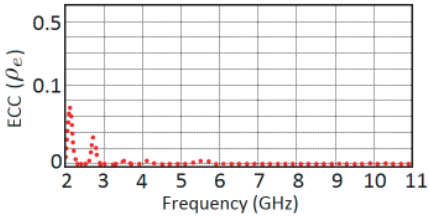

Figure 19. Envelop Correlation factor (ECC) of the proposed antenna (Figure 17).

reduction in mutual coupling for antenna with cross-strip VFSS.

Based on simulation results, the proposed base antenna is fabricated and tested for its S-parameter characteristic, antenna gain, radiation pattern and envelop correlation factor for validating pass/stop bandwidths and antenna diversity characteristics.

Figure 18 shows that with cross-strip VFSS, the mutual coupling between antennas is very low. It also depicts that the dual pass-band (Bluetooth/UWB) and dual band-notch characteristics of the proposed antenna are unaffected. The isolation response i.e., S_{21} is measured in an enclosed anechoic chamber (as used for measuring radiation pattern and gain response), using low lossy high frequency cables. It can be seen that measured and simulated S_{21} responses are in good agreement.

Isolation between antenna elements in the proposed structures is also validated by evaluating Envelop Correlation coefficient (ECC (ρ_e)) for complete bandwidth (2–11 GHz). ECC is the measure of correlation factor between antennas. It measures the degree of similarity between antenna radiation patterns. If ECC (ρ) = 1, it means that the radiation pattern of two antennas are similar. For ECC calculation, a simple S-

parameter based equation given in [23] is used:

$$\rho_e = \frac{\left|S_{11}^* S_{12} + S_{21}^* S_{22}\right|^2}{\left[1 - \left(\left|S_{11}\right|^2 + \left|S_{21}\right|^2\right)\right]\left[1 - \left(\left|S_{22}\right|^2 + \left|S_{12}\right|^2\right)\right]} \tag{5}$$

As depicted in Figure 19, the correlation factor [calculated using Equation (5)] of the proposed structure is less than 0.5 for complete Bluetooth/UWB bandwidths.

This indicates the non-correlation behavior between the proposed antenna elements. The channel capacity loss of the proposed antenna is also analyzed using equations given in [24]:

$$C_{loss} = -\log_2 \det\left(C_r\right) \tag{6}$$

$$Correlation\text{-}matrix\left(C_r\right) = \begin{pmatrix} \rho_{11} & \rho_{12} \\ \rho_{21} & \rho_{22} \end{pmatrix} \tag{7}$$

$$\text{Were} \quad \rho_{ii} = 1 - \left(\left|S_{ii}\right|^2 + \left|S_{ij}\right|^2\right), \quad \rho_{ij} = -\left(S_{ii}^* S_{ij} + S_{ji}^* S_{jj}\right) \tag{8}$$

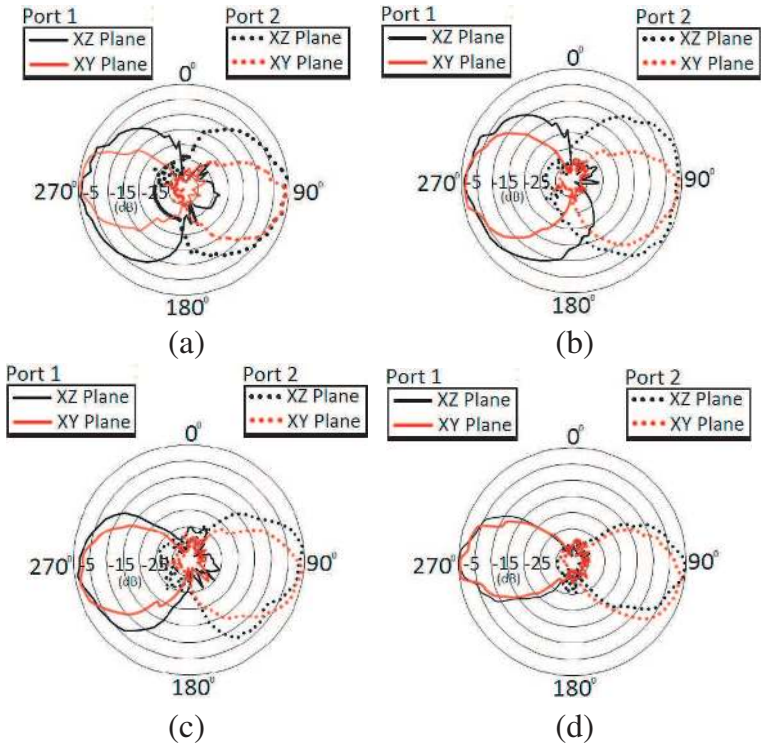

Figure 20. Measured Radiation pattern (dB), (a) 2.45 GHz, (b) 5 GHz, (c) 7 GHz, (d) 10 GHz.

According to Equations (6), (7) and (8), the capacity loss (C_r) is less than 0.3 bps/Hz for both Bluetooth and UWB bandwidths, which also makes the proposed antenna suitable for diversity application. For the further analysis on diversity, the radiation patterns for both antennas (Via port 1 and 2) are measured. The radiation patterns are measured in two principle planes i.e., XY and XZ.

Patten measurements are carried out by making one port active while the other is terminated to 50 Ω matched impedance. As shown in Figure 20, the proposed antenna holds a good diversity and less correlation with a nearly directional pattern in two principle planes. Due to this directive nature, gain and efficiency of the proposed antenna are high as shown in Figure 21.

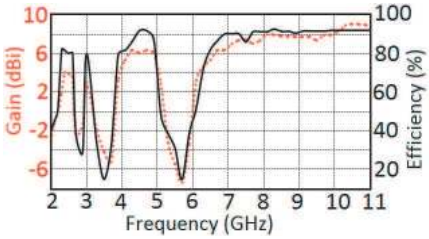

Figure 21. Measured gain and efficiency of the proposed antenna (antenna 1/port 1).

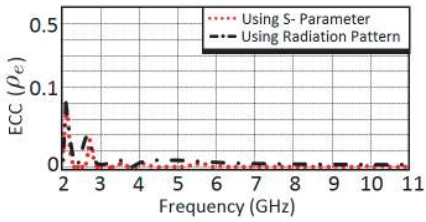

Figure 22. Comparison of calculated ECC.

Here gain and efficiency are measured for antenna 1 (via port 1), while antenna 2 (port 2) is terminated with 50 Ω matched impedance. Since the two antennas are identical, similar gain and efficiency characteristics are expected from antenna 2. It can be seen that for Bluetooth and lower UWB bands, the gain of diversity antenna shown in Figure 21 is similar to the gain of individual dual-band antenna (Figure 7). This is because both Bluetooth and lower UWB band are followed by sharp band-notches; this affects the gain of nearby pass bands. For further validation of diversity characteristic, ECC is again calculated using measured antenna radiation pattern. As given in [23], radiation pattern via both the ports are considered as:

$$\rho_e = \frac{\left| \iint\limits_{4\pi} \left[\overrightarrow{F_1}(\theta,\phi) \cdot \overrightarrow{F_2}(\theta,\phi)\, d\Omega \right] \right|^2}{\left| \iint\limits_{4\pi} \left[\overrightarrow{F_1}(\theta,\phi)\, d\Omega \right] \right|^2 \left| \iint\limits_{4\pi} \left[\overrightarrow{F_2}(\theta,\phi)\, d\Omega \right] \right|} \tag{9}$$

Here $\overrightarrow{F_1}(\theta,\phi)$ is the field radiation pattern of the antenna when port 1 is excited and $(\cdot)$ is the hermetian product. Considerations for

calculating ECC using Equation (9) are similar to those in [10, 11, 24]. According to [23], Equation (5) is the simplified form (with S-parameter equivalent considerations) for Equation (9); therefore ECC calculated using both the equations should be comparable.

As shown in Figure 22, the correlation factor calculated using both the techniques is similar. It can be seen that ECC calculated using radiation pattern parameters also indicates good diversity behavior (ECC < 0.5) for complete dual bandwidth.

Compared to existing pattern diversity antenna [10–14], the proposed structure provides compactness, wide dual-pass bandwidth, sharp cutoff for dual band-notch characteristics and low mutual coupling with high diversity. These intrinsic properties make the proposed antenna highly suitable for dual-band diversity applications.

4. CONCLUSIONS

A stage-wise realization of compact Bluetooth/UWB dual-band antenna with dual band-notch characteristic for antenna diversity application is presented. The measured impedance bandwidth i.e., VSWR < 2 validates the dual-pass band with WiMAX and WLAN band-notch nature of the proposed antenna. The gain and radiation pattern of individual dual-band antenna are stable throughout the impedance band width. The high isolation performance of $S_{21} < -25$ dB between coplanar antenna elements is achieved by introducing cross-strip VFSS structure. The diversity performance of the proposed antenna is analyzed through ECC, channel capacity loss and antenna radiation pattern. It is observed that with low return loss and high isolation, ECC of $\rho_e < 0.5$ and capacity loss, i.e., $C_r < 0.3$ bps/Hz, is achieved for complete Bluetooth and UWB bandwidths. Even with diversity configuration, the proposed antenna exhibits a stable radiation pattern and high gain response throughout dual bandwidth. A diverse radiation pattern with low mutual coupling and low ECC ensures the suitability of proposed antenna for dual-band diversity applications.

REFERENCES

1. FCC, "Federal Communication Commission revision of part 15 of commission's rules regarding ultra — Wideband transmission systems," First Report and Order FCC, Washington, DC, Vol. 48, 2002.
2. Wu, Z. H., F. Wei, X.-W. Shi, and W.-T. Li, "A compact quad band-notched UWB Monopole antenna loaded one lateral

L-shaped slot," *Progress In Electromagnetics Research*, Vol. 139, 303–315, 2013.

3. Azim, R. and M. T. Islam, "Compact planar UWB antenna with band notch characteristics for WLAN and DSRC," *Progress In Electromagnetics Research*, Vol. 133, 391–406, 2013.
4. Li, C.-M. and L.-H. Ye, "Improved dual band-notched UWB slot antenna with controllable notched bandwidth," *Progress In Electromagnetics Research*, Vol. 115, 477–493, 2011.
5. Xu, J., D. Shen, X. Zang, and K. Wu, "A compact disc UWB antenna with quintuple band rejections," *IEEE Antenna and Wireless Propagation Letters*, Vol. 11, 1517–1520, 2012.
6. Nguyen, D. T., D. H. Lee, and H. C. Park, "Very compact triple band-notch UWB antenna with quarter wavelength slots," *IEEE Antenna and Wireless Propagation Letters*, Vol. 11, 411–415, 2012.
7. Liu, X. L., Y.-Z. Yin, P. A. Liu, J. H. Wang, and B. Xu, "A CPW-fed dual band-notched UWB antenna with a pair of bended dual-L-shape parasitic branches," *Progress In Electromagnetics Research*, Vol. 136, 623–634, 2013.
8. Lin, C. C., P. Jin, and R. W. Ziolkowski, "Single dual and tri-band notch UWB antenna using capacitively loaded loop resonators," *IEEE Transactions on Antennas and Propagation*, Vol. 60, 102–110, 2012.
9. Islam, M. T., R. Azim, and A. T. Mobashsher, "Triple band-notched planar UWB antenna using parasitic strips," *Progress In Electromagnetics Research*, Vol. 129, 161–179, 2012.
10. Xiong, L., and P. Gao, "Compact dual-band printed diversity antenna for WiMAX/WLAN applications", *Progress In Electromagnetics Research C*, Vol. 32, 151–165, 2012.
11. Mao, C.-X., Q.-X. Chu, Y.-T. Wu, and Y.-H. Qian, "Design and investigation of closely-packed diversity UWB slot-antenna with high isolation," *Progress In Electromagnetics Research C*, Vol. 41, 13–25, 2013.
12. Zhang, S., J. Ying, and S. He, "UWB MIMO/diversity antenna with a tree like structure to enhance wideband isolation," *IEEE Antenna and Wireless Propagation Letters*, Vol. 8, 1279–1283, 2009.
13. Terence, S. P. and Z. H. Chen, "An UWB diversity antenna," *IEEE Transactions on Antennas and Propagation*, Vol. 59, No. 6, 1597–1606, 2012.
14. Gallo, M., et al., "A broad band pattern diversity annular slot antenna," *IEEE Transactions on Antennas and Propagation*,

Vol. 60, No. 3, 1596–1601, 2012.

15. Zuo, S., Y.-Z. Yin, W.-J. Wu, Z.-Y. Zhang, and J. Ma, "Investigations of reduction of mutual coupling between two planar monopoles using two $\lambda/4$ slots," *Progress In Electromagnetics Research Letters*, Vol. 19, 9–18, 2010.
16. Islam, M. T. and M. S. Alam, "Compact EBG structure for alleviating mutual coupling between patch antenna array elements," *Progress In Electromagnetics Research*, Vol. 137, 425–438, 2013.
17. Mishra, S. K., et al, "A compact dual band Fork shaped UWB antenna for Bluetooth and UWB applications," *IEEE Antenna and Wireless Propagation Letters*, Vol. 10, 627–630, 2011.
18. Li, W. T., Y. Q. Hei, W. Fang, and X. W. Shi, "Planar antenna for 3G/Bluetooth/WiMAX applications with dual band-notch characteristic," *IEEE Antenna and Wireless Propagation Letters*, Vol. 11, 61–65, 2012.
19. Yildirim, B. S., B. A. Cetiner, G. Roqueta, and L. Jofre, "Integrated bluetooth and UWB antenna," *IEEE Antennas and Wireless Propagation Letters*, Vol. 8, 149–152, 2009.
20. Yildirim, B. S, "Low profile and plannar antenna for blurtooth/WLAN and UWB application," *IEEE Antennas and Wireless Propagation Letters*, Vol. 5, 438–441, 2006.
21. Kumar, G. and K. P. Ray, *Broad-band Microstrip Antenna*, Arctech House, Norwood, MA, 2003.
22. Bilotti, F., A. Toscano, and L. Vegni, "Design of spiral and multiple SRR for the realization of miniaturized metamaterial sample," *IEEE Transactions on Antennas and Propagation*, Vol. 59, No. 6, 2258–2268, 2012.
23. Blanch, S., J. Romeu, and I. Corbella, "Exact representation of antenna system diversity performance from input parameter description," *Electronic Letters*, Vol. 39, No. 9, 705–707, 2003.
24. See, C. H., et al., "Compact MIMO/diversity antenna for portable mobile UWB applications," *IET Microwave and Antenna Propagation Letters*, Vol. 7, No. 6, 444–451, 2013.